Human Thioredoxin Homodimers: Regulation by pH, Role of Aspartate 60, and Crystal Structure of the Aspartate 60 → Asparagine Mutant[†,‡]

John F. Andersen,[§] David A. R. Sanders,[§] John R. Gasdaska,[||] Andrzej Weichsel,[§] Garth Powis,[||] and William R. Montfort*,[§]

Department of Biochemistry and Arizona Cancer Center, University of Arizona, Tucson, Arizona 85721

Received April 30, 1997; Revised Manuscript Received August 28, 1997[⊗]

ABSTRACT: Thioredoxins are a group of ca. 12 kDa redox proteins that mediate numerous cytosolic processes in all cells. Human thioredoxin can be exported out of the cell where it has additional functions including the ability to stimulate cell growth. A recent crystal structure determination of human thioredoxin revealed an inactive dimeric form of the protein covalently linked through a disulfide bond involving Cys 73 from each monomer [Weichsel et al. (1996) *Structure 4*, 735−751]. In the present study, apparent dissociation constants (K_{app}) for the noncovalently linked dimers were determined at various pHs using a novel assay in which preformed dimers, but not monomers, were rapidly linked through oxidation (with diamide) of the Cys 73 disulfide bond, and the relative amounts of monomer and dimer were detected by gel filtration. The values obtained were pH-dependent, varying between 6.1 and 166 μM for the pH range of 3.8−8.0, and were consistent with the titration of a single ionizable group having a pK_a of 6.5. A similar value was obtained using gel filtration at pH 3.8 (K_{app} = 164 μM), and the crystal structure of the diamide-oxidized protein was determined to be nearly identical to that obtained in the absence of diamide. Asp 60 lies in the dimer interface and was found to be responsible for the pH dependence for dimer formation, and therefore must have a pK_a elevated by ∼2.5 pH units. Mutation of Asp 60 to asparagine abolished nearly all of the pH dependence for dimer formation. The crystal structure of the D60N mutant revealed a dimer nearly identical to the wild type, but, surprisingly, it had the Asn 60 side chain rotated out of the dimer interface and replaced with two water molecules. The values obtained for K_{app} suggest human thioredoxin may dimerize *in vivo* and possible roles for such dimers are discussed.

The redox protein thioredoxin is involved in numerous cellular processes including activation of ribonucleotide reductase, activation of the transcription factor NF-κB, and regulation of photosynthesis [reviewed in Eklund et al. (1991) and Holmgren (1995)]. Several lines of evidence suggest human thioredoxin also serves as an extracellular growth factor and plays a role in the promotion of a variety of tumors [reviewed in Powis et al. (1996)]. The adult T-cell leukemia-derived factor (ADF)[1] produced by human lymphocytes transformed with human T-lymphotrophic virus type I has been identified as thioredoxin (Fujii et al., 1991), and human primary solid tumors from lung (Gasdaska et al., 1994) and colon (Berggren et al., 1997) overexpress thioredoxin. Thioredoxin can stimulate cell growth in several human solid tumor cell lines, both in cell culture (Gasdaska et al., 1995) and in *scid* mice (Baker et al., 1997; Gallegos et al., 1996), suggesting that the growth-promoting activity of thioredoxin is quite general. Mechanistically, growth stimulation by thioredoxin is not well understood, but a functional active-site dithiol is required for the activity (Gasdaska et al., 1995, 1996). Thioredoxin can apparently be exported from the cell through a leaderless secretion pathway (Ericson et al., 1992; Rubartelli et al., 1992). Thioredoxin has also been reported to be a component of the early pregnancy factor signaling pathway, in a mechanism that requires surface thiol Cys 73 but not active-site thiols Cys 32 and Cys 35 (Tonissen et al., 1993).

All thioredoxins can serve as general protein disulfide oxidoreductases and can reduce disulfide bonds in a variety of proteins. The mechanism for reduction involves a disulfide exchange between reduced active-site amino acids Cys 32 and Cys 35 of thioredoxin and the target disulfide bond, resulting in a disulfide bond between Cys 32 and Cys 35 and two free sulfhydryls in the target protein. Reduced thioredoxin is regenerated via thioredoxin reductase, again through disulfide bond exchange, and thioredoxin reductase is autoreduced in a mechanism involving NADPH and FAD.

Surprisingly, the recently determined crystal structure of human thioredoxin revealed the presence of a dimeric form of the protein in which the two active-sites were buried and the two halves of the dimer were disulfide-linked through Cys 73 from each monomer (Weichsel et al., 1996; shown in Figure 1). This disulfide bond was apparently quite stable as it occurred despite the presence of 5 mM dithiothreitol

[†] This work was supported in part by National Institutes of Health Grants T32 CA09213 (J.F.A), HL54826 (W.R.M), CA48725 (G.P.), and CA17094 (G.P.); American Cancer Society Grant DHP-45 (W.R.M.); Arizona Disease Control Research Commission Grant 1-208A (W.R.M.); and The V Foundation for Cancer Research (J.R.G.).

[‡] The final coordinates for the diamide-oxidized and D60N mutant thioredoxin structures have been deposited with the Brookhaven Protein Data Bank (entry numbers 1auc and 1aiu).

* Corresponding author: Department of Biochemistry, University of Arizona, Tucson, AZ 85721. Tel (520) 621-1884; Fax (520) 621-1697; E-mail montfort@u.arizona.edu.

[§] Department of Biochemistry.

[||] Arizona Cancer Center.

[⊗] Abstract published in *Advance ACS Abstracts,* October 15, 1997.

[1] Abbreviations: ADF, adult T-cell leukemia-derived factor, D60N Asp 60 → Asn mutant thioredoxin; DTT, dithiothreitol; FPLC, fast protein liquid chromatography; DMEM, Dulbecco's modified Eagle medium; IPTG, isopropyl β-D-thiogalactopyranoside; HEPES, *N*-(2-hydroxyethyl)piperazine-*N*′-2-ethanesulfonic acid.

S0006-2960(97)01004-0 CCC: $14.00

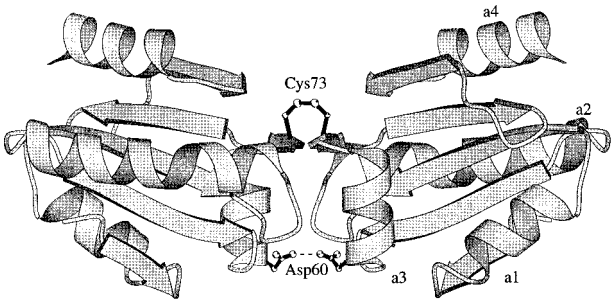

FIGURE 1: Ribbon drawing of the disulfide-linked human thioredoxin homodimer. The four thioredoxin helices are labeled a1−a4. Carbons are indicated for residues Cys 73 and Asp 60 as small spheres; oxygens and sulfurs, as large spheres. The disulfide bond between Cys 73 of each monomer is indicated by a solid line, and the hydrogen bond between Asp 60 of each monomer is shown by a dashed line. Figure was drawn with MOLSCRIPT (Kraulis, 1991).

(DTT), a concentration sufficient to keep the active-site sulfhydryls fully reduced over the course of crystallization and X-ray diffraction experiments (a period of several days). Buried in the dimer interface is a surface area of approximately 1100 Å^2. The interface is largely hydrophobic but also contained a short two-stranded β sheet that served to align Cys 73 from each monomer in an optimal arrangement for disulfide bond formation. That dimer formation did not require disulfide bond formation was also clear, as the crystal structure of the Cys 73 → Ser mutant (C73S) was determined and found to be nearly identical to the wild-type structure except for the replacement of the disulfide bond with a hydrogen bond between the introduced serines (Weichsel et al., 1996).

Disulfide-linked thioredoxin dimers can also occur in solution. Concentrated solutions of wild-type thioredoxin, but not the C73S mutant thioredoxin, readily form disulfide-linked dimers when stored in the absence of reductant (Weichsel et al., 1996) or when oxidized with diamide (Gasdaska et al., 1996). A presumably identical dimer has been observed with bovine thioredoxin (Holmgren, 1977) and human thioredoxin oxidized with selenodiglutathione (Ren et al., 1993). Dimer formation in the latter study could be abolished by conversion of Cys 73 to serine. Crude extracts from human lymphoid cell lines probed with antibody have also been reported to have both monomeric and dimeric forms of thioredoxin (Wollman et al., 1988).

The data outlined above suggest the dimeric form of thioredoxin may have a physiological function. To address this possibility, we have measured the apparent dissociation constant for wild-type human thioredoxin dimers under reducing conditions, as occurs *in vivo*, using a novel assay involving rapid oxidation of the Cys 73 disulfide bond in preformed dimers and separation of disulfide-linked dimers from monomers by gel filtration. We have also investigated the pH dependence for dimer formation of both wild-type thioredoxin and the Asp 60 → Asn mutant form of the protein. In the wild-type crystal structure, which was determined at pH 3.8, Asp 60 of one monomer was hydrogen-bonded across the dimer interface to Asp 60 of the other monomer (Figure 1). Dimer formation at physiological pH would have to overcome the electrostatic repulsion between the two Asp 60s if this residue exhibited the usual pK_a for aspartates of approximately 4. Dimer formation was found to be pH-dependent in these experiments and to occur at a thioredoxin concentration similar to that expected to occur *in vivo*. The crystal structure of the D60N mutant was also determined and found to have a much greater rearrangement near the mutation site than predicted from model building.

MATERIALS AND METHODS

Construction of D60N Mutant. The D60N mutant of human thioredoxin was constructed from wild-type cDNA in pBluescript KS using the Sculptor kit (Amersham, version 2.1). The oligonucleotide used for introduction of the mutation was 5′-GTAGATGTGAATGACTGTCAG-3′. Dideoxy sequencing was used to confirm the presence of the mutation. Novel *Nde*I and *Bam*HI restriction sites were introduced into the cDNA at the 5′ and 3′ ends, respectively. The *Nde*I−*Bam*HI fragment was ligated into the pET-3a expression vector (Novagen) and the sequence of the insert was confirmed by dideoxy sequencing. *Escherichia coli* (BL21) cells were transformed with this plasmid and mutant thioredoxin was expressed and purified as described below.

Thioredoxin Purification. Recombinant thioredoxin was purified in a manner similar to previously published studies (Wollman et al., 1988). *E. coli* strains containing mutant and wild-type thioredoxin plasmids (Oblong et al., 1994) were grown to $A_{600} = 0.6$ in LB medium and induced with IPTG (0.4 mM). After 3 h of growth at 37 °C, the cells were harvested, collected by centrifugation, washed in 0.9% NaCl, and suspended in 50 mM Tris-HCl, pH 7.5, 30 mM NaCl, 5.0 mM DTT, and 0.2 mM PMSF (buffer A). The cells were lysed by sonication and the soluble cytosol was isolated by centrifugation at 80000*g*. For the wild-type protein the supernatant was applied to a Q-Sepharose column equilibrated with buffer A. The column was eluted with a gradient of 0−0.5 M NaCl in buffer A, and the thioredoxin-containing fractions were pooled, concentrated by precipitation with 85% saturation ammonium sulfate, and centrifuged at 20 000 rpm. The pellet was dissolved in 50 mM Tris-HCl, pH 7.5, 200 mM NaCl, and 5 mM DTT (buffer B) and applied to a Superose 12 (Pharmacia) gel-filtration FPLC column. This column was eluted at a flow rate of 0.5 mL/min with buffer B and the thioredoxin-containing fractions were pooled and concentrated by ultrafiltration through a 3000 molecular weight cutoff filter (Amicon) and rechromatographed on the Superose 12 column. The final fractions were pooled and concentrated to 40−50 mg/mL, and the buffer was exchanged for 5.0 mM HEPES, pH 7.5, and 5 mM DTT. The D60N mutant protein was purified in a similar manner except that ion-exchange chromatography was performed on Mono-Q (Pharmacia, eluted with 0−250 mM NaCl in buffer A), concentration after ion exchange was performed by ultrafiltration (3000 molecular weight cutoff filter, Amicon), and gel filtration was performed on a Superdex 75 (Pharmacia) FPLC column.

Functional Assays. Human placenta thioredoxin reductase [specific activity 43.6 μmol of thioredoxin reduced min^{-1} (mg of protein)$^{-1}$] was prepared as previously described (Oblong et al., 1993). Reduction of wild-type and D60N thioredoxin was measured by observing the oxidation of NADPH at 340 nm with insulin as the final electron acceptor (Luthman & Holmgren, 1982).

Cell growth studies were performed with MCF-7 breast cancer cells obtained from the American Type Culture Collection (Rockville, MD), maintained for 2 days in Dulbecco's modified eagle medium (DMEM) containing 10% fetal bovine serum or thioredoxin, and compared to a

control containing no additions. Cell numbers were measured with a hemacytometer and all incubations were conducted in triplicate.

Diamide Oxidation Assay. Stock thioredoxin at a concentration of 40−50 mg/mL containing 5 mM DTT was found to remain monomeric when stored at −20 °C. This stock solution was diluted into buffers of various pH and incubated at room temperature for 5 min. Diamide [1,1′-azobis(*N*,*N*-dimethylformamide)] in aqueous solution was added to the protein mixture and incubated for at least 5 min. The buffers used for the reactions were 10 mM NaOAc, pH 3.8; 10 mM NaOAc, pH 5.0; 10 mM NaOAc, pH 5.4; 10 mM sodium citrate pH 6.0; 10 mM sodium citrate, pH 6.5; 10 mM Tris-HCl, pH 7.3; and 10 mM Tris-HCl, pH 8.0. The products of diamide oxidation were diluted to a concentration of 25 μM thioredoxin (as dimer) or less and injected via a 500 μL injection loop onto a Superose 12 HR 10/30 gel-filtration column equilibrated with 50 mM Tris-HCl, pH 7.3, and 200 mM NaCl and eluted at a flow rate of 0.5 mL/min. At this injection concentration and pH, the noncovalent interactions between monomers are weak. The eluent was monitored by absorption at 280 nm. On the basis of peak area, we found the molar extinction coefficient for cross-linked thioredoxin to be twice that of the monomeric species.

Analysis of Dimerization Data. The data for the fraction of thioredoxin as dimer obtained as a function of thioredoxin concentration were analyzed to determine apparent dissociation constants (K_{app}). The dimerization process was treated with a model assuming a single dissociation constant:

$$K_d = [M]^2/[D] = 4 f_m^2 C_T/(1 - f_m) \quad (1)$$

where [M] is the concentration of monomer, [D] is the concentration of dimer, f_m is the fraction of the total thioredoxin as monomer, and C_T is the total thioredoxin concentration as dimer (Valdes & Ackers, 1979; Weber, 1992). A nonlinear least-squares procedure was used to determine K_{app} by fitting the data in terms of percent dimer formed to a solution of quadratic equation 2 (Manning et al., 1996):

$$\% D = [(8C_T + K_{app}) - (K_{app}^2 + 16K_{app}C_T)^{1/2}]/0.08C_T \quad (2)$$

Data were fitted with the Marquardt−Levenberg algorithm in the program SigmaPlot (Jandel Scientific).

In the experiments where higher concentrations of diamide were used, the maximal percentage dimer obtained was well below 100% (see Figure 5 and Results). In order to fit the data to eq 2, the data were first normalized to make the maximum percentage dimerization equal to 100%. To accomplish this, the value for the maximal percentage dimer formed was obtained by fitting the data to a rectangular hyperbolic function:

$$\% D = D_{max}C_T/(K_{1/2} + C_T) \quad (3)$$

where $K_{1/2}$ is the dimer concentration at half-maximal percentage dimerization and D_{max} is the maximum percentage dimer formed. The normalized values for percent dimer formed were then obtained by multiplying by $(100/D_{max})$, and K_{app} was determined by fitting the normalized data to eq 2.

The pK_a for the pH-dependent change in K_{app} was determined by nonlinear regression using an equation similar to that for a standard titration curve:

$$K_{app} = [K_{appmin} + (K_{appmax}10^{pH-pK_a})]/(1 + 10^{pH-pK_a}) \quad (4)$$

where the parameters fitted were K_{appmin} and K_{appmax}, the asymptotic minima and maxima of K_{app}, and the pK_a for the transition (Langsetmo et al., 1991). This treatment assumes that the range of K_{app} (that is, $K_{appmax} - K_{appmin}$) reflects the titration range of the group of interest and allows calculation of the pK_a as the midpoint inflection of the function.

Gel-Filtration Assay. Gel-filtration FPLC was used to estimate the dissociation constant of wild-type thioredoxin dimers using the methods of Manning (1996). A 6 mM (dimer) wild-type thioredoxin stock solution was prepared in 10 mM Tris-HCl, pH 7.5, and 10 mM DTT. The lack of covalent linkage in this solution was verified by SDS−PAGE. Dilutions were prepared from the stock using either 50 mM NaOAc, pH 3.8, or Tris-HCl, pH 8.0, containing 200 mM NaCl. All dilutions were brought to a final volume of 100 μL and injected via a 100 μL injection loop onto a Superose 12 FPLC column that had been previously equilibrated to the pH of interest. The eluent of the column was monitored by UV absorption at 280 nm and the degree of dimerization was estimated by analysis of the retention volume−concentration relationship using the following algorithm:

$$\% D = 100(2^{(V_m-V)/(V_m-V_d)} - 1) \quad (5)$$

where V_m, V_d, and V are the elution volumes of the monomer, the covalent dimer, and the peak of interest [see Manning et al. (1996) for derivation]. A factor of 15-fold was used to correct for dilution of the protein on the column. This value was determined as the retention volume at half of the peak height divided by the injection volume (Manning et al., 1996).

Structure Determinations. The D60N mutant thioredoxin was crystallized using the hanging drop vapor diffusion method with 10 mM NaOAc, pH 3.8, 5 mM DTT, and 50% (v/v) 2-methyl-2,4-pentanediol (MPD), as described previously for the wild-type protein (Weichsel et al., 1996). Crystals of the diamide-oxidized wild-type protein were obtained by adding diamide (14.5 mM) to a 20 mg/mL protein solution (10 mM NaOAc, pH 3.8, and 5 mM DTT) 30−60 min prior to preparing the crystallization drop. The well buffer contained 18% PEG 4000 and 200 mM NaOAc (pH 4.5) and was mixed 1:1 with the protein solution. The resulting crystals were isomorphous with crystals grown in MPD (Weichsel et al., 1996) or in the absence of diamide (Sotelo-Mundo and Montfort, manuscript in preparation).

X-ray diffraction data were measured with a FAST area detector using an Enraf-Nonius FR571 rotating anode as the X-ray source. Intensities were processed with the programs MADNES (Messerschmidt & Pflugrath, 1987), PROCOR (Kabsch, 1988), and Agrovata/Rotovata (CCP4, 1994).

The structures were determined using difference Fourier techniques with the reduced wild-type human thioredoxin structure as an initial model (Weichsel et al., 1996). Refinements were performed using the simulated annealing and minimization procedures in X-PLOR (Brunger, 1987). Rebuilding of the models was performed with O (Jones et al., 1991). Superpositioning of wild-type and mutant struc-

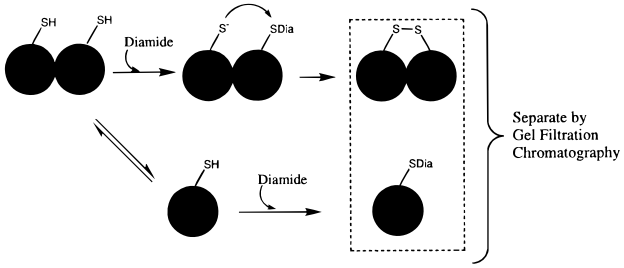

FIGURE 2: Schematic illustration of the assay used to quantitate dimer formation. Each monomer is indicated by a solid circle.

tures as well as measurement of interatomic distances were performed using INSIGHTII (MSI/Biosym), and general crystallographic calculations were performed with the CCP4 program suite (CCP4, 1994).

RESULTS

A New Assay for Detecting Noncovalent Dimer Formation: Oxidation with Diamide. The formation of human thioredoxin dimers has two components, noncovalent association through a protein interface and disulfide linkage through Cys 73 of each monomer. In the experiments described below, we have estimated the dissociation constant for human thioredoxin under highly reducing conditions, where the Cys 73−Cys 73 disulfide bond is disfavored. The values obtained are expected to reflect dimer formation in the cytosol of cells, which is also highly reducing. The dissociation constant under oxidizing conditions, as occurs in the extracellular matrix, has not been addressed in the present study but is expected to be considerably lower since the disulfide bond is quite stable.

In what follows, we first describe our assay and present data to establish the reliability of the method. We then report dissociation constants determined under a variety of conditions.

Our method for estimating the dissociation constant for noncovalently linked dimers, referred to below as noncovalent dimers, is based on the ability of diamide to oxidize free dithiols to form disulfides (Kosower & Kosower, 1995). High concentrations of human thioredoxin will slowly form Cys 73 disulfide-linked homodimers in solution if reductant is withheld (Weichsel et al., 1996). Diamide accelerates this process (Gasdaska et al., 1996), apparently through a two-step mechanism where a covalent adduct is first formed between diamide and Cys 73 of one subunit of a noncovalently linked homodimer, followed by displacement of diamide by Cys 73 of the other subunit (Kosower & Kosower, 1995; illustrated in Figure 2). After oxidation, the thioredoxin dimer can be detected by SDS−PAGE (Gasdaska et al., 1996) and as a distinct peak in the eluent from a Superose 12 gel-filtration column (Figure 3). We confirmed that the diamide-oxidized dimer was the same as that previously observed in the crystal (Figure 1) by determining the crystal structure of the oxidized material (described below) and by demonstrating that the mutant protein Cys 73 → Ser (C73S) does not form appreciable amounts of covalent dimer when exposed to diamide (Gasdaska et al., 1996; J.F.A., unpublished observations). However, at pHs above 6.0 and concentrations greater than 250 μM (as dimer),[2] small amounts of other dimeric forms are seen as faint bands in SDS−PAGE experiments and as a small leading shoulder in gel-filtration chromatograms (not shown).

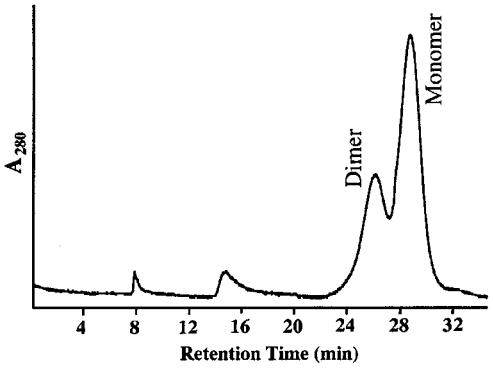

FIGURE 3: Chromatogram showing the separation of monomeric and dimeric forms of thioredoxin on Superose 12 gel-filtration medium.

In our assay, diamide oxidation is used to trap the equilibrium monomer/noncovalent dimer ratio that occurs in solution under a given set of conditions, and the amount of each form is determined using gel-filtration chromatography (Figures 2 and 3). In this assay, thioredoxin is allowed to preequilibrate in the presence of reductant, followed by addition of excess diamide. All solvent-accessible sulfhydryls are rapidly modified under the conditions used, but diamide modification of a sulfhydryl that lies near a second sulfhydryl, as occurs for Cys 73 in the noncovalent dimer, can lead to disulfide bond formation through nucleophilic attack by the free sulfhydryl in a process that is also fast. In contrast, sulfhydryls that are not near a second sulfhydryl, as occurs for Cys 73 in monomeric thioredoxin, react with diamide before encountering a diamide-oxidized sulfhydryl, since the concentration of diamide is much higher than that of thioredoxin. Thus, diamide oxidation traps the equilibrium monomer/dimer ratio that occurs under a given set of solution conditions. The monomeric and dimeric proteins are then separated by gel-filtration FPLC, their relative amounts are determined by integration of A_{280} peak areas, and an apparent dissociation constant (K_{app}) is determined from plots of percent dimer vs thioredoxin concentration (see Materials and Methods for details of the algorithm used). This method allows thioredoxin dimerization to be measured under numerous conditions using relatively small quantities of protein.

Reliability of the Assay. To demonstrate that diamide oxidation provides a reliable estimate of the monomer/dimer solution ratio, several possible interactions and reactions must be considered, as illustrated in Figure 4. The value we wish to measure is K_d, the noncovalent dimer dissociation constant for thioredoxin, which we are estimating through oxidation with diamide. For this estimate to be accurate, three conditions must be satisfied: (1) diamide-independent covalent dimer formation must be slow, (2) modification of monomers by diamide must be irreversible, and (3) formation of diamide-induced disulfide bonds must be rapid with respect to dissociation and occur only for preformed dimers. Under these conditions, rate constants k_1, k_{-1}, k_1', k_{-1}', and k_2 in Figure 4 can be ignored, and the percentage of covalent dimer formed by diamide oxidation will directly reflect the equilibrium ratio of monomer and noncovalent dimer.

The rate of spontaneous disulfide bond formation (k_2) was monitored by SDS−PAGE and found to be negligible over

[2] Thioredoxin concentrations reported throughout this paper are for the dimeric protein (molecular mass = 23.4 kDa), since the algorithms used to estimate the dimer dissociation constants were derived on the basis of dimer concentrations.

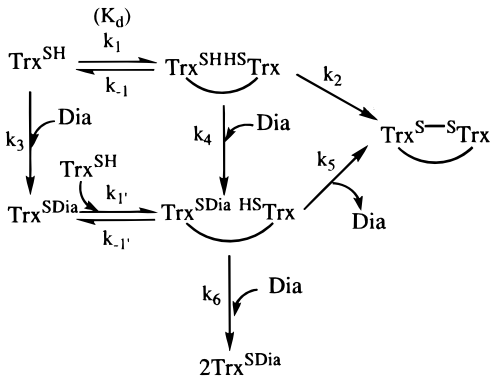

FIGURE 4: Reaction scheme illustrating the relevant intermediates and rate constants in the dimerization assay. Trx^{SH} = reduced thioredoxin; Trx^{SDia} = diamide-modified thioredoxin; $Trx^{SHHS}Trx$ = unmodified noncovalent dimer; $Trx^{SDiaHS}Trx$ = singly modified noncovalent dimer; $2Trx^{SDia}$ = doubly modified noncovalent dimer; $Trx^{S-S}Trx$ = disulfide-linked dimer. An arc connecting monomer symbols indicates a noncovalent association.

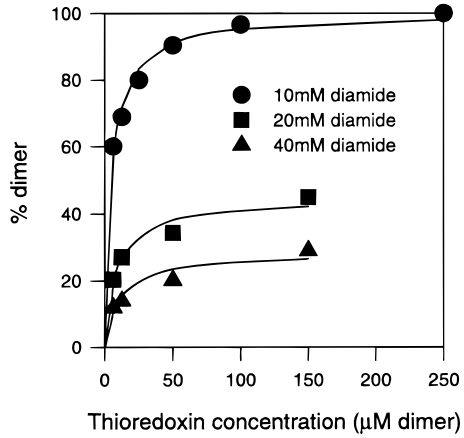

FIGURE 5: Dependence of covalent dimerization on thioredoxin and oxidant concentration at pH 5.0. The curves shown are for fitting of the data to rectangular hyperbolas (eq 3, Materials and Methods). Values for K_{app} at each diamide concentration (see text) were obtained by normalizing the values for maximal dimerization to 100% and fitting the normalized data to eq 2.

a period of hours to days when stored at the concentrations and pHs used to determine dissociation constants but in the absence of both diamide and DTT (data not shown). In contrast, the reaction with diamide is complete within 5 min and the resulting ratio of monomer to dimer remains constant for 150 min at room temperature, indicating that diamide-modified monomers do not undergo further reaction to form dimers. Thus, conditions 1 and 2 are satisfied.

To address point 3, that noncovalent dimer association/dissociation rates (k_1, k_{-1}, k_1', and k_{-1}') are slow with respect to diamide oxidation of monomers and dimers (k_3, k_4, and k_6) and to diamide-dependent disulfide bond formation (k_5), we evaluated covalent dimer formation at three different diamide concentrations (Figure 5). Covalent dimer formation at all three diamide concentrations displayed the typical saturation behavior expected for a process governed by simple equilibria. At higher diamide concentrations the reaction of a second diamide molecule with singly modified noncovalent dimers (k_6) became competitive with the reaction for diamide-dependent disulfide bond formation (k_5), and saturation was reached at less than 100% dimer. Since typical saturation behavior and similar saturation curves occurred for all three diamide concentrations, oxidation must have been fast with respect to other processes such as dimer association/dissociation, and the oxidation products therefore reflect the preoxidation monomer/dimer ratio, as required by point 3.

Table 1: Crystallographic Parameters for Diamide-Oxidized and Mutant D60N Thioredoxins

	oxidized	D60N
space group	C2	C2
a (Å)	67.8	68.4
b (Å)	26.3	26.8
c (Å)	51.6	52.2
β (deg)	95.13	95.02
Data Collection		
resolution	26 - 2.1	15 - 2.0
total reflections	8553	15528
unique reflections	5391	5545
completeness (%)		
overall	98.2	85.7
outermost shell	94.4	75.3
R_{sym}[a]	0.027	0.038
mean $I/\sigma(I)$		
overall	18.8	10.4
outermost data shell	7.9	8.4
Refinement		
R_{cryst}[b]	0.19	0.18
R_{free}[c]	0.28	0.24
rms deviation		
bond lengths (Å)	0.007	0.014
bond angles (deg)	1.1	1.7
no. of solvent molecules	43	52
average *B* factor (Å^2)	26	18

[a] R_{sym} = *R*-factor for symmetry-related intensities. [b] R_{cryst} = Crystallographic *R*-factor. Calculated without reflections used in R_{free}. [c] R_{free} = *R*-factor for a randomly selected 10% of reflections not included in the refinement, as implemented in X-PLOR (Brunger, 1987).

Estimating K_d. Since covalent dimer formation was dependent on only the initial noncovalent dimer concentration (governed by K_d), the concentration of diamide, and the rates k_4, k_5, and k_6 (Figure 4), the covalent dimer saturation curves could be used to determine K_{app}, the apparent K_d. The curves were fitted to an equation derived from a simple equilibrium expression (eq 2 in the Materials and Methods section) to yield K_{app}. For the data measured at pH 5.0 (Figure 5), K_{app} was 6 ± 1, 19 ± 3, and 24 ± 6 μM, respectively, for diamide concentrations of 10, 20, and 40 mM. The true noncovalent dimer K_d therefore appears to lie between 6 and 24 μM at pH 5.0. Since 10 mM diamide gave the highest saturation level of dimer, resulting in the highest degree of sensitivity for the detection of dimerization, this concentration was used for subsequent experiments. In addition, since 100% dimer could be reached in the presence of 10 mM diamide, normalization was not required for these data.

Crystal Structure of Diamide-Oxidized Thioredoxin. To ensure that diamide oxidation resulted in thioredoxin dimers similar to those formed in the absence of diamide, we determined the crystal structure of the oxidized material. Crystals formed very rapidly, suggesting that cross-linking the thioredoxin dimers facilitated crystal formation (see Materials and Methods for details). The crystals were isomorphous with those grown in the absence of diamide and led to a well-refined structure at 2.1 Å nominal resolution (Table 1).

As expected, the diamide-oxidized crystal structure was nearly identical to that of thioredoxin crystallized in the absence of diamide (Weichsel et al., 1996). The disulfide bond between Cys 73 of each monomer was clearly visible in the $2F_o - F_c$ electron density map (Figure 6). Cys 62

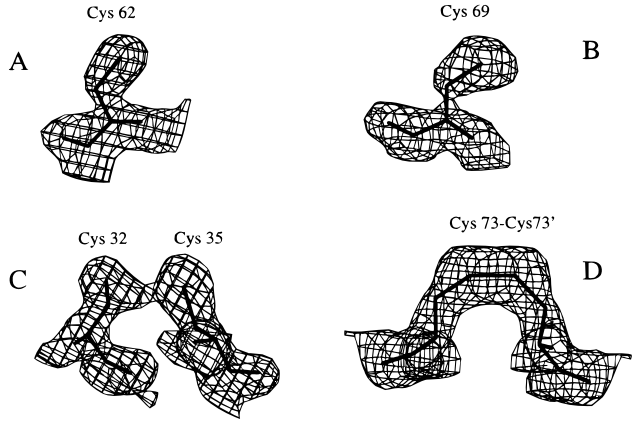

FIGURE 6: Electron density for cysteines in the diamide-oxidized crystal structure. Shown is the electron density for all five cysteines in the final $2F_o - F_c$ electron density map, at a level of 1σ. Figure was drawn with O (Jones et al., 1991).

and Cys 69 were free of oxidation, which is not surprising given the bulky nature of diamide and the largely buried side chains of the two residues. Cys 69 displayed a small amount of disorder, and the α and β carbons of Trp 31 displayed extensive disorder, in the final model. Similar disorder was also observed in the reduced human thioredoxin structure (Weichsel et al., 1996).

Interestingly, the active-site sulfhydryls of Cys 32 and Cys 35 were nearly free of oxidation (Figure 6C). In the dimeric protein, Cys 32 is buried in the dimer interface, and Cys 35 is buried in the active-site. In the monomeric protein, Cys 32 is exposed and the presence of diamide should lead to oxidation of the Cys 32−Cys 35 disulfide bond. The absence of Cys 32 oxidation could only occur if thioredoxin were dimeric during the entire experiment, from the initial incubation with diamide through crystallization. This is the expected result based on the initial concentration of thioredoxin in the experiment (0.8 mM dimer) and the apparent dissociation constant described above. The slight oxidation of the active-site dithiol (∼10%) was probably due to the lack of reductant during crystallization, since diamide was added, by necessity, in excess of DTT.

Measurement of Dimerization by Gel Filtration. Noncovalent dimerization was also directly measured by gel-filtration FPLC on Superose 12, using the procedure of Manning et al. (1996), to further assess the reliability of the diamide assay. The retention volume in this assay provides a measure of the equilibrium monomer/dimer ratio as the protein travels through the column. If the equilibrium is shifted in favor of dimer, the peak elutes in a smaller volume than under conditions where monomer is favored. Increasing concentrations of thioredoxin were injected onto the column in volumes of 100 μL, pH 3.8. The percent dimerization was calculated using eq 5 (see Materials and Methods), and the data were analyzed by nonlinear regression using eq 2. A plot of percent dimer vs concentration displayed the expected saturation behavior (Figure 7), although the fit at higher concentrations was worse than at lower concentrations and did not reach 100%. The K_{app} value obtained by this procedure was 164 ± 14 μM (dimer), 7−24 fold higher than that obtained by diamide oxidation at pHs 3.8 (described below) and 5.0 (described above). Thus this method is in general agreement with the results of the diamide assay and suggests the values obtained for K_{app} in the diamide assay are likely to be accurate to at least within an order of magnitude.

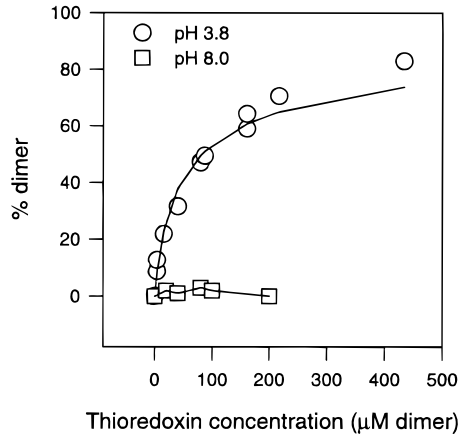

FIGURE 7: Relationship of dimer formation to wild-type thioredoxin concentration as measured by gel-filtration FPLC on Superose 12. Experiments were performed as described in the text using elution buffers at pH 3.8 and 8.0.

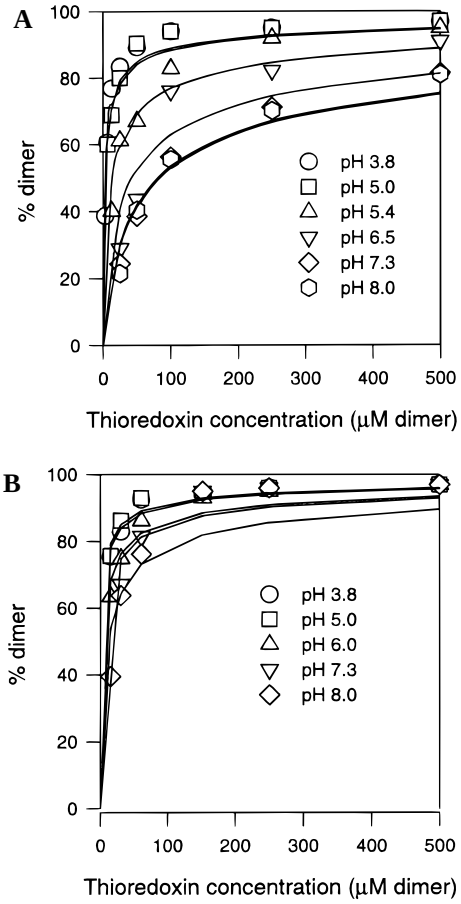

FIGURE 8: Thioredoxin noncovalent dimer formation as a function of concentration and pH, as estimated through diamide oxidation. (A) Wild type; (B) D60N mutant. Lines represent fitting of the data to eq 2 using SigmaPlot.

pH Dependence of Dimerization. We examined the effect of pH on dimerization of wild-type thioredoxin to assess the role of the Asp 60−Asp 60 hydrogen bond found in the wild-type crystal structure (see introduction and Figure 1). As shown in Figure 8A and Table 2, K_{app} increased 27-fold over the pH range of 3.8−8.0, indicating a decrease in binding energy

$$\Delta\Delta G = -RT \ln [K_{app}(\text{pH } 3.8)/K_{app}(\text{pH } 8.0)] \quad (6)$$

of 2 kcal/mol.

Table 2: Apparent Dimer Dissociation Constants[a] Estimated by Diamide Oxidation at Various pHs

pH	wild-type	D60N
3.8	6.1 ± 1.3[a]	3.7 ± 0.7
5.0	5.4 ± 0.9	3.2 ± 0.6
5.4	27 ± 6.	-
6.0	-	9 ± 2
6.5	86 ± 32	-
7.3	159 ± 25	10 ± 4
8.0	166 ± 28	23 ± 9

[a] K_{app} values (micromolar) ± SE are shown. [b] Calculated by nonlinear regression fitting of data in Figure 8 to eq 2.

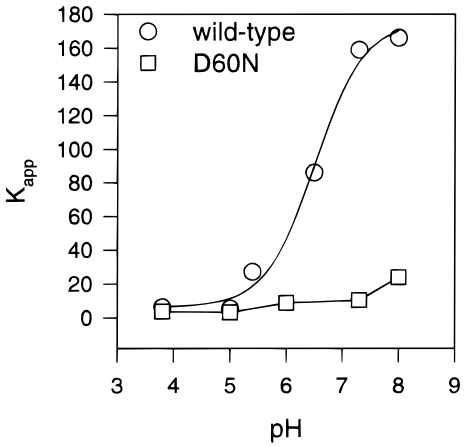

FIGURE 9: Plot of K_{app} vs pH for wild-type and D60N human thioredoxins. Data for the wild-type protein were fitted to eq 3 using SigmaPlot.

A fit of the K_{app} values obtained at each pH to an equation describing a titration curve (eq 4, Materials and Methods) revealed a single ionizable group with a pK_a of 6.5 ± 0.1 was responsible for the observed shift in K_{app} (Figure 9). The most likely group to serve this function is the side chain of Asp 60, since deprotonation at higher pH would lead to electrostatic repulsion between the two Asp 60s juxtaposed in the dimer interface. Such a mechanism would require the pK_a of Asp 60 to be elevated approximately 2.7 pH units above that of free aspartate (3.8). The fit of the dimerization equilibrium model to K_{app} is poorer at intermediate pH values than at either high or low pH (Table 2), possibly reflecting the heterogeneity brought about by the mixed protonation state of Asp 60 in this range.

That the pH dependence was not an artifact of diamide oxidation was verified by a gel-filtration measurement of dimerization at pH 8.0. Over a concentration range of 20−200 μM (after correction for dilution), no shift in the retention volume of the thioredoxin peak was observed (Figure 7), indicating that the protein remains largely monomeric at this pH.

Dimerization of the D60N Mutant. To assess whether Asp 60 was responsible for the pH dependence for dimerization, we prepared a mutant protein in which Asp 60 was changed to asparagine (D60N), reasoning that the isosteric Asn 60 would retain the ability to hydrogen-bond across the dimer interface but remain neutral at all pHs. We measured dimerization for the D60N mutant over the same pH range as the wild-type protein and found the proteins to have similar values for K_{app} at lower pHs (Figures 8B and 9 and Table 2). However, only a modest 6.2-fold increase in K_{app} occurred in the D60N mutant at higher pHs, confirming that Asp 60 was responsible for most of the pH dependence in the wild-type protein. The calculated difference in binding energy at pH 8.0 for the mutant and wild-type proteins was $\Delta\Delta G = 1.2$ kcal/mol, or 60% of the difference for the high and low pH values of the wild-type protein. Again, the fit to eq 2 was poorer as the pH increased, suggesting increasing heterogeneity in the system.

We attempted to estimate K_{app} using the gel-filtration technique, but unlike with the wild-type protein (Figure 7), the D60N mutant behaved anomalously. Specifically, the fit of the data to eq 2 indicated a maximal shift in retention volume that was much smaller than that indicated by the retention volume of the covalently cross-linked dimer. The reason for this is unclear, but it may be due to a specific interaction of the monomeric protein with the column matrix. The D60N mutant behaved similarly at both pH 3.8 and 8.0, but the fit of the data to eq 2 was not of sufficient quality to derive K_{app} values (data not shown).

The mutant protein behaved nearly identically to wild type with respect to catalytic activity (reduction of insulin) and ability to stimulate growth of cultured breast cancer cells at low thioredoxin concentrations. Kinetic parameters for wild-type thioredoxin as a substrate for thioredoxin reductase, with insulin as the final electron acceptor, were $K_m = 0.33$ μM and $V_{max} = 5.9$ nmol (min·mg of protein)$^{-1}$. For the D60N mutant, the values were $K_m = 0.48$ μM and $V_{max} = 4.3$ nmol (min·mg of protein)$^{-1}$. The stimulatory effect on the growth of MCF-7 human breast cancer cells was similar for the wild-type and mutant proteins, with maximal stimulation achieved at a concentration of approximately 1 μM thioredoxin monomer (data not shown).

Crystal Structure of the D60N Mutant. We determined the crystal structure of the D60N mutant to examine the changes that occurred on mutating the dimer interface. The D60N mutant crystallized in a manner similar to the wild-type protein but had unit cell parameters ~1% larger than the wild-type crystals. Data were measured to 2.0 Å nominal resolution and analyzed using the structure of the reduced wild-type protein as a starting model (Table 1). Like the wild type, the mutant crystallized as a covalent dimer with a single monomer in the asymmetric unit. The overall structure was very similar to that of the wild type and displayed an RMS deviation in Cα positions with the monomeric starting model of 0.2 Å after refinement. The active-site sulfhydryl groups of Cys 32 and Cys 35 were clearly reduced, and the disulfide bond joining Cys 73 from the two monomers in the dimer was clearly present.

The major differences between the mutant and wild-type structures occurred in the vicinity of the mutation. Surprisingly, a series of negative and positive peaks in the difference electron density map (Figure 10) indicated new positions for the side chains of Asn 60 and Asp 58 in the mutant protein, as well as a general shift in helix a3 (shown in Figure 1). Electron density was also present for four new water molecules in the dimer interface.

Figure 11 displays the final model for residues near Asn 60 in the mutant and wild-type proteins. In the mutant, Asn 60 has rotated out of the dimer interface into the solvent, and, on the basis of the poor electron density for the side chain in the final $2F_o - F_c$ electron density map, occupied multiple positions in the crystal. The two Asn 60s in the dimer are still close to one another, but unlike the wild-type protein, they do not hydrogen-bond. The side chain of Asp 58, which was hydrogen-bonded to both side- and main-chain atoms of Asp 60 in the wild-type protein, has shifted ~0.8 Å in the mutant protein, partially filling the gap created

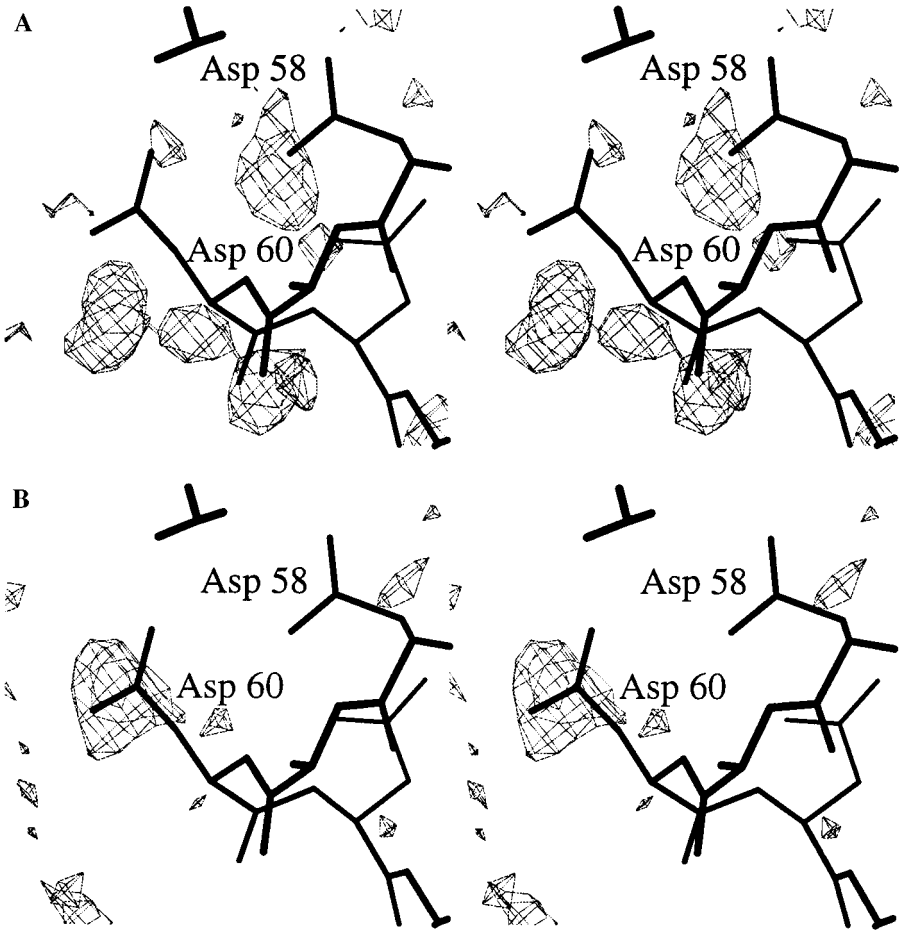

FIGURE 10: Stereoview of the difference Fourier electron density map ($F_{D60N} - F_{WT}$, ϕ_{WT}) of the region surrounding residue 60 of human thioredoxin, contoured at a 4σ level. (A) Positive density; (B) negative density. Figure was drawn with O (Jones et al., 1991).

by the new position for Asn 60. Backbone atoms for helix a3, which contains Asn 60 and Asp 58, also shifts by ~0.5 Å. The remainder of the gap in the dimer interface created by the new position for Asn 60 is filled with four new water molecules, two per Asn 60 (Figure 11). The first of these, Wa_1D58, is in roughly the same position as the carboxylate of the wild-type Asp 60 and forms hydrogen bonds with Asp 58 (3.1 Å), Thr 30 (3.0 Å), and the second water molecule, Wa_1T30 (2.8 Å). Wa_1T30 also forms a strong hydrogen bond with Thr 30 (2.5 Å), and a weak hydrogen bond with Gln 63 of the other monomer (3.3 Å, not shown).

Two other factors serve to enlarge the cavity occupied by Wa_1T30 and Wa_1D58. First, there is a slight overall expansion of the dimeric structure by ~0.4 Å, which undoubtedly led to the slightly larger unit cell dimensions for the mutant protein. For example, the main-chain atoms of residues Asp 20, Glu 103, and His 43 of one monomer in the mutant dimer are all about 0.4 Å further from their counterparts in the other monomer than was found in the wild-type structure. The second factor affecting cavity size is the position for Trp 31, which, along with Cys 32, is part of the active-site loop that shifts to a "closed" position on formation of the Cys 32−Cys 35 disulfide bond (Weichsel et al., 1996). This loop is shifted toward a more "open" conformation than in the reduced wild-type structure, with the Trp 31 backbone shifting ~0.6 Å, and the side chain, which lies in the dimer interface, shifting ~0.9 Å (Figure 11). Met 74, which lies in the dimer interface, has also adopted a new conformation in the mutant protein. Thus, despite exchanging only one oxygen for a nitrogen, significant differences in three-dimensional structure occurred in the mutant protein.

DISCUSSION

Dimerization of Thioredoxin. The formation of redox-inactive covalently linked dimers of human thioredoxin has been noted in several instances but the functional significance of the dimer form is not known (Gasdaska et al., 1995, 1996; Ren et al., 1993; Wollman et al., 1988). We demonstrate here that dimer formation can occur in solution in the absence of covalent bond formation and that this dimer is more stable at low pH than neutral pH, due to the close proximity of two Asp 60 amino acids in the dimer interface. The apparent dissociation constant for noncovalent dimer formation (K_{app}) ranged from 6 to 166 μM for the pH range of 3.8−8.0. Under more oxidizing conditions, where the disulfide-linked dimer could form and influence the monomer/dimer equilibrium, the dissociation constant would most likely be considerably lower. The concentration of thioredoxin in mammalian tissue has not been accurately determined but has been estimated to be 0.5−5 μM dimer in bovine tissue (Holmgren & Luthman, 1978). Many cancerous tissues overexpress thioredoxin (Berggren et al., 1997; Gasdaska et al., 1994; Nakamura et al., 1992; Teshigawara et al., 1985), suggesting that such cells may reach a thioredoxin concentration where the dimeric form of the protein predominates.

To estimate the noncovalent dimer dissociation constant (K_d), we have developed an assay that relies on rapid oxidation of the disulfide bond present in the covalent dimer. The advantages of this assay include high reproducibility,

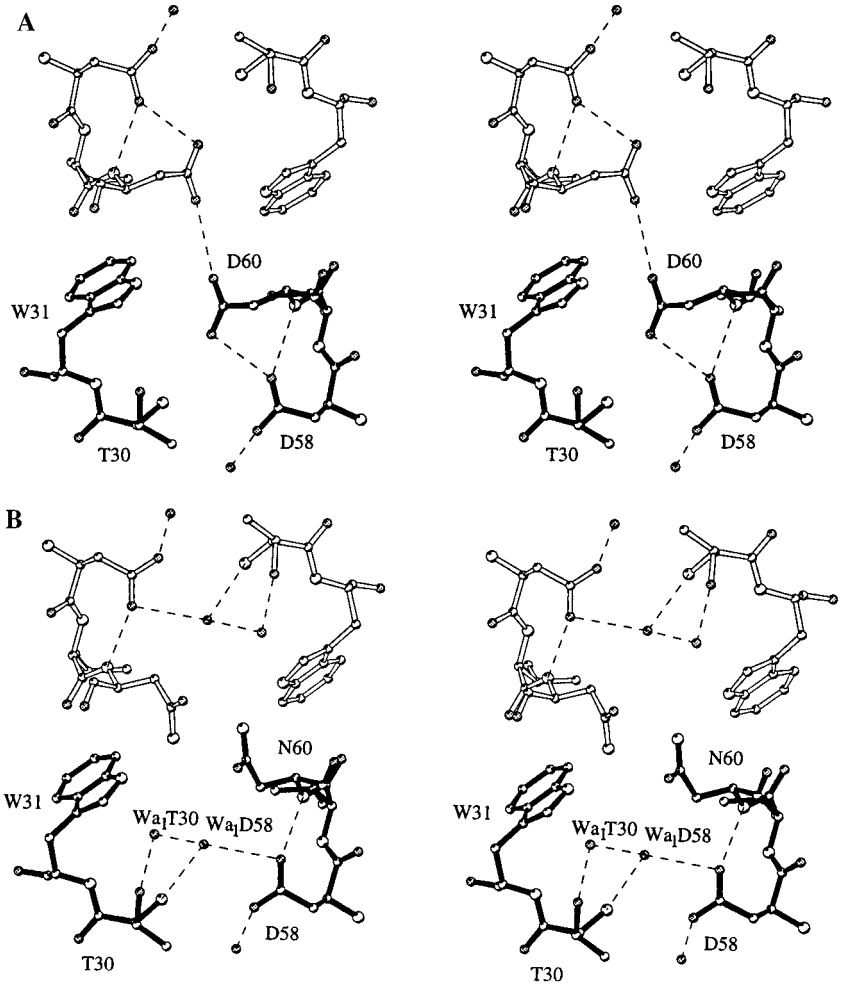

FIGURE 11: Stereoview of the atoms in the dimer interface near residue 60 of (A) wild-type and (B) D60N mutant thioredoxins. Solid bonds indicate one monomer, and open bonds the other monomer, in the disulfide-linked dimer. Oxygens are indicated as stippled spheres, nitrogens as larger spheres, and water molecules as isolated spheres. Hydrogen bonds are indicated with dashed lines. Figure was drawn with MOLSCRIPT (Kraulis, 1991).

the need for only modest amounts of protein, and the ability to conduct experiments under a wide variety of conditions. A gel-filtration assay was used to validate the assay (Manning et al., 1996; Valdes & Ackers, 1979) and was found to give K_{app} values that were within an order of magnitude of the higher estimates obtained with the diamide assay. We also determined the crystal structure of the diamide-oxidized protein, which resulted in a structure nearly identical to that obtained in the absence of diamide (Weichsel et al., 1996). The structure showed a disulfide bond linking the two monomers but revealed the active-site dithiol to be largely reduced. This could only occur if the active-site was inaccessible to diamide, as occurs in dimeric thioredoxin where the active-site is buried in the dimer interface. Therefore, at pH 3.8 and approximately 0.8 mM thioredoxin dimer (the conditions of the experiment) the protein is nearly all dimeric, consistent with the result obtained in the diamide cross-linking assay used to estimate K_{app}.

pH Dependence of Dimerization. We have demonstrated that dimer formation for the wild-type protein is destabilized by $\sim$ 2 kcal/mol at neutral pH versus pHs below 5, due in large part to the presence of Asp 60 in the dimer interface. The pK_a for the Asp 60 carboxylate was estimated to be 6.5 on the basis of the pH dependence for dimer formation (Figure 9), a value approximately 2.7 pH units above that for free aspartate. The pK_as of Asp 58, Asp 60, and Asp 61 were previously estimated using NMR methods for a human thioredoxin containing four mutations [C62S, C69S, C73S, and M74T (Qin et al., 1996)]. They were unable to assign individual pK_as to these three amino acids due to the non-Henderson−Hasselbalch behavior displayed by the aspartate cluster, but a simultaneous fitting to a three pK_a model gave values of 2.8, 4.2, and 5.3 for the group (Qin et al., 1996). In the wild-type dimer, both Asp 58 and Asp 61 are more solvent-exposed than Asp 60 and would be expected to have lower pK_a values, so the highest of the three values may be assignable to Asp 60. The elevated value of 5.3 found in the NMR study is lower than the pK_a attributed to Asp 60 in this study, but as Met 74 lies in the dimer interface, the mutated protein used in the NMR study may dimerize less well and therefore exhibit a different pK_a for Asp 60.

The pK_a values for the Asp 58, Asp 60, and Asp 61 cluster were found to decrease significantly when a C35S thioredoxin mutant in a mixed disulfide complex with a peptide fragment of NFκB was examined by NMR (Qin et al., 1996). This was interpreted as being due to stabilization of the negative charges by the guanidinium group of a neighboring arginine residue in the peptide fragment. A contributing factor may also have been the disruption of dimer formation by the bound NFκB peptide, whose binding site is coincident with the dimer interface.

Crystal Structure of the D60N Mutant. The mutation made in this study was among the most conservative possible. In the wild-type structure determined at pH 3.8, the protonated side chain of Asp 60 from one monomer was hydrogen-bonded across the dimer interface to the protonated side chain

of Asp 60 of the second monomer. Mutation of residue 60 to asparagine resulted in the simple exchange of an OH for an NH_2, a change that was both isosteric and preserved the residue 60 hydrogen-bonding capability. However, instead of the essentially flat difference electron density map we expected to see, the D60N mutant crystals revealed a new position for residue 60, numerous small shifts near the mutation site, the incorporation of four new water molecules in the dimer interface, and a slight expansion of the overall dimer. The reasons for this are not at all clear at present.

Asp 60 is one of the few residues outside of the immediate vicinity of the active-site that is conserved across all taxa (Eklund et al., 1991). While prokaryotic thioredoxins cannot form covalent dimers due to lack of an analogue to Cys 73, and appear not to form noncovalent dimers in solution, Asp 60 may serve another essential role in thioredoxin function, such as the interaction with redox partners.

Possible Biological Roles of the Dimer Form. What is the biological role of this easily formed dimer? Recently discovered extracellular growth factor-like activities of human thioredoxin suggest that the dimer could play a specific role in the oxidizing conditions outside of the cell (Fujii et al., 1991; Gasdaska et al., 1995; Powis et al., 1994). This role could involve the inhibition of normal thioredoxin activities by eliminating redox function or acquisition of a specific activity that is unique to the dimer form. The dimeric form of thioredoxin cannot stimulate cell growth since the active-site, which is required for growth stimulation, is blocked. Maximal growth stimulation is achieved at about 1 μM thioredoxin for both the wild-type and D60N mutant proteins, well below the concentration required for noncovalent dimer formation. However, in the oxidizing extracellular environment, thioredoxin may form irreversible covalent dimers with time, which would serve to limit the growth stimulation signal.

Among the possible functions unique to the dimer form would be a mechanism for sensing oxidative stress in tissues or a protective mechanism for the active-site of the protein during secretion (Ericson et al., 1992; Rubartelli et al., 1992). The pH dependence could play a role in the latter function if low-pH vesicles are involved in the secretory pathway.

Although no functions have been specifically ascribed to the dimer form, one activity has been shown to depend on the presence of a thiol group at Cys 73. Thioredoxin is a component of the early pregnancy factor system (Tonissen et al., 1993). While mutation of active-site residues has no effect on the activity, mutation of Cys 73 to Ser abolishes it completely. The levels of thioredoxin necessary for activity in this system are far lower than the apparent noncovalent dimerization constant of the wild-type protein obtained in this study. Nevertheless, the dimer could potentially play a role as a catalytic intermediate in a redox activation reaction involving the Cys 73 thiol group.

Cys 73 is conserved in all mammalian thioredoxins examined to date but is not seen in proteins from bacteria, plants, or invertebrates (Eklund et al., 1991). The data presented here indicate that thioredoxin dimers probably form in physiologically relevant situations and their presence would affect the redox environment of the cell.

REFERENCES

Baker, A., Payne, C. M., Briehl, M. M., & Powis, G. (1997) *Cancer Res*. (in press).

Berggren, M., Gallegos, A., Gasdaska, J. R., Gaskaska, P. Y., Warneke, J., & Powis, G. (1997) *Anti-Cancer Res*. (in press).

Brunger, A. T., Kuriyan, J., & Karplus, M. (1987) *Science 235*, 458−460.

CCP4 (1994) *Acta Crystallogr. D50*, 760−763.

Eklund, H., Gleason, F. K., & Holmgren, A. (1991) *Proteins: Struct., Funct., Genet. 11*, 13−28.

Ericson, M. L., Horling, J., Wendel-Hansen, V., Holmgren, A., & Rosen, A. (1992) *Lymphokine Cytokine Res. 11*, 201−207.

Fujii, S., Nanbu, Y., Nonogaki, H., Konishi, I., Mori, T., Masutani, H., & Yodoi, J. (1991) *Cancer 68*, 1583−1591.

Gallegos, A., Gasdaska, J. R., Taylor, C. W., Paine-Murrieta, G. D., Goodman, D., Gasdaska, P. Y., Berggren, M., Briehl, M. M., & Powis, G. (1996) *Cancer Res. 56*, 5765−5770.

Gasdaska, P. Y., Oblong, J. E., Cotgreave, I. A., & Powis, G. (1994) *Biochim. Biophys. Acta 1218*, 292−296.

Gasdaska, J. R., Berggren, M., & Powis, G. (1995) *Cell Growth Differ. 6*, 1643−1650.

Gasdaska, J. R., Kirkpatrick, D. L., Montfort, W. R., Kuperus, M., Hill, S. R., Berggren, M., & Powis, G. (1996) *Biochem. Pharmacol. 52*, 1741−1747.

Holmgren, A. (1977) *J. Biol. Chem. 252*, 4600−4606.

Holmgren, A. (1995) *Structure 3*, 239−243.

Holmgren, A., & Luthman, M. (1978) *Biochemistry 17*, 4071−4077.

Jones, T. A., Zou, J. Y., Cowan, S., & Kjeldgaard, M. (1991) *Acta Crystallogr. 47*, 110−119.

Kabsch, W. (1988) *J. Appl. Crystallogr. 21*, 916−934.

Kosower, N. S., & Kosower, E. M. (1995) *Methods Enzymol. 251*, 123−133.

Kraulis, P. J. (1991) *J. Appl. Crystallogr. 24*, 946−950.

Langsetmo, K., Fuchs, J. A., Woodward, C., & Sharp, K. A. (1991) *Biochemistry 30*, 7609−7614.

Luthman, M., & Holmgren, A. (1982) *Biochemistry 21*, 6628−6633.

Manning, L. R., Jenkins, W. T., Hess, J. R., Vandegriff, K., Winslow, R. M., & Manning, J. M. (1996) *Protein Sci. 5*, 775−781.

Messerschmidt, A., & Pflugrath, J. W. (1987) *J. Appl. Crystallogr. 20*, 306−315.

Nakamura, H., Masutani, H., Tagaya, Y., Yamauchi, A., Inamoto, T., Nabu, Y., Fujii, S., Ozawa, K., & Yodoi, J. (1992) *Cancer 69*, 2091−2097.

Oblong, J. E., Gasdaska, P. Y., Sherrill, K., & Powis, G. (1993) *Biochemistry 32*, 7271−7277.

Oblong, J. E., Berggren, M., Gasdaska, P. Y., & Powis, G. (1994) *J. Biol. Chem. 269*, 11714−11720.

Powis, G., Oblong, J. E., Gasdaska, P. Y., Berggren, M., Hill, S., & Kirkpatrick, D. L. (1994) *Oncol. Res. 6*, 539−544.

Powis, G., Kirkpatrick, D. L., Angulo, M., Gasdaska, J. R., Powell, M. B., Salmon, S. E., & Montfort, W. R. (1996) *Anti-Cancer Drugs 7* (Suppl. 3), 121−126.

Qin, J., Core, G. M., & Gronenborn, A. M. (1996) *Biochemistry 35*, 7−13.

Ren, X., Bjornstedt, M., Shen, B., Ericson, M. L., & Holmgren, A. (1993) *Biochemistry 32*, 9701−9708.

Rubartelli, A., Bajetto, A., Allavena, G., Wollman, E., & Sitia, R. (1992) *J. Biol. Chem. 267*, 24161−24164.

Teshigawara, K., Maeda, M., Nishino, K., Nikaido, T., Uchiyama, T., Tsudo, M., Wano, Y., & Yodoi, J. (1985) *J. Mol. Cell. Immunol. 2*, 17−26.

Tonissen, K., Wells, J., Cock, I., Perkins, A., Orozco, C., & Clarke, F. (1993) *J. Biol. Chem. 268*, 22485−22489.

Valdes, R. J., & Ackers, G. K. (1979) *Methods Enzymol. 61*, 125−142.

Weber, G. (1992) *Protein Interactions*, Chapman and Hall, New York.

Weichsel, A., Gasdaska, J. R., Powis, G., & Montfort, W. R. (1996) *Structure 4*, 735−751.

Wollman, E. E., d'Auriol, L., Rimsky, L., Shaw, A., Jacquot, J.-P., Wingfield, P., Graber, P., Dessarps, F., Robin, P., Galibert, F., Bertoglio, J., & Fradelizi, D. (1988) *J. Biol. Chem. 263*, 15506−15512.

BI971004S